Floral Precision: Investigating Pea (Pisum sativum L.) Flowering with High Throughput Field Phenotyping and Object Detection

Corina Oppliger

corina.oppliger@usys.ethz.ch

ETH Zurich

Beat Keller

ETH Zurich

Radek Zenkl

ETH Zurich

Achim Walter

ETH Zurich

Research Article

Keywords:

Posted Date: September 4th, 2024

DOI: https://doi.org/10.21203/rs.3.rs-4860776/v1

Additional Declarations: No competing interests reported.

Floral Precision: Investigating Pea (*Pisum sativum* L.) Flowering with High Throughput Field Phenotyping and Object Detection

Corina Oppliger[1*], Beat Keller[1], Radek Zenkl[2], and Achim Walter[1]

[1]Crop Science Group, Institute of Agricultural Sciences, ETH Zurich, Switzerland
[2]Plant Pathology Group, Institute of Integrative Biology, ETH Zurich, Switzerland
[*]Address correspondence to: corina.oppliger@usys.ethz.ch

August 8, 2024

Abstract

Background

Flowering is one of the most important and sensitive process throughout a plants life as it marks the start of the reproductive phase. Therefore, phenotyping the continuous development of flowering is crucial for crop breeding. For phenotyping, visual ratings have been a standard method for decades, to observe flowering dynamics by determining timepoints, such as start, end or duration. However, high throughput field phenotyping (HTFP) methods have emerged, providing an objective and efficient approach. We developed an approach that allows to collect detailed data not only about pea flowering dynamics, but additionally flower intensity (flowers per area). For this purpose, an object detection model, based on YOLOv8 was trained on RGB-images. The images were automatically acquired by the field phenotyping platform (FIP) of ETH Zürich for 12 pea breeding lines over two years.

Results

The trained model reached high accuracy for open flower detection, which allowed to monitor flower dynamics and intensity over time. Flower intensity throughout the development of the plants was highly correlated (R^2= 0.967) to ground truth data taken in the field. Clear differences in timing, intensity of flowering and fruiting efficiency were detected between breeding lines and years. Furthermore, high correlation between maximal flower numbers and yield components such as seed amount were observed.

Conclusion

This automated, data-driven method of flower detection proved itself as a reliable tool. This is promising for the use of RGB imaging methods to objectively assess not only timing but also flower intensity. Flower intensity allows to predict seed amount and has therefore potential as

selection trait in breeding program. In addition, fruiting efficiency could be included in breeding programs.

1 Introduction

Recently, grain legumes have gained attention in the global north: Due to their ability to fix nitrogen and their nutritional value, they offer potential to contribute to a more sustainable food system [1, 2]. Legume-based proteins allow replacing livestock-based protein production with benefits for human health and CO_2 footprint of agriculture [3–5]. However, integrating more legumes into cropping systems in central Europe has limited success, while better adapted varieties could increase the legume cultivation area. To breed for site-adapted varieties, different vegetation stages need to be investigated under various field conditions. For most crops, data collection is still mostly done manually by visual ratings, even though it is labor-intense and often lacks objectivity [6]. Today, image-based High Throughput Field Phenotyping (HTFP) methods can provide automated and unbiased data on various growth stages of plants, such as the emergence, flowering or senescence dynamics, demonstrated on various crops, e.g. [6, 7]. In case of flowering, recent image-based HTFP approaches were mostly designed to investigate flowering dynamics (e.g., start or ending of flowering) but lacked the necessary resolution to detect flower intensity. The ability to investigate flower intensity in field testing could improve breeding for fruiting efficiency or serve as early indicator for grain yield.

Flowering is an important trait in plant breeding, as it is one of the most important processes throughout a crop's life. It marks the transition from vegetative to reproductive growth [8] and therefore marks the beginning of yield building. In grain legumes it is known, that the senescence of leaves is often associated with a decrease in nitrogen fixation in the roots [9]. As this is also the period when grain filling takes place, most of the nitrogen that is stored as protein in the seeds has to be taken up before senescence starts (i.e. before flowering). How yield and/or protein content in the grain is influenced by the flower intensity or dynamics is not known in detail, also because methods have been lacking to quantify precisely. The timepoint of flowering is an indicator of how well a species is adapted to a particular location [10], which is important in the context of finding varieties that are better adapted to future climates.

As Jiang et al. [6] stated, one major challenge in flowering characterisation is that it occurs over a long period, and therefore frequent measurement and detection is required. Evaluators must traverse fields with hundreds of breeding lines and keep track of the open flowers. Compared to other traits like height, flower characteristic evaluation is time-consuming since it is a dynamic trait. To establish onset, peak or end of flowering, an evaluator should conduct at least two to three weekly ratings, preferably every two days. In addition, it is almost impossible to quantify flowering i.e. determine flower intensity - the number of open flowers in an area - purely based on human assessment in a big experiment. Hence, not much is known about the flower intensity of different pea breeding lines. It is known, also from other legumes, that exposure to thermal stress, including heat or cold,

as well as drought during the reproductive stages, can result in the failure of flowers and pods to develop, ultimately leading to significant in grain yield losses [11–13]. Thus, it is important to breed for and identify varieties or breeding lines with flowering times adapted to the given environment and lower abortion rate of reproductive organs. However, to get detailed insights in the plants response to environmental factors, i.e. to quantify the abortion of flowers due to environmental stressors, reliable data on reproductive organs is needed. Since manual data collection is limiting, it seems unrealistic to collect data of single flowers based solely on manual ratings. Here, image-based HTFP methods can provide options for data collection.

Collecting detailed information about flowering with image-based HTFP faces challenges, especially in field conditions. Das Choudhury et al. introduced a technique for single flower detection, relying on deep neural networks and multiview images [14]. However, this approach has been proven in greenhouse condition on single plants and is not directly applicable in field testing of dense sown crops. Under field conditions, HTFP methods often rely on Unmanned Aerial Vehicles (UAV) to capture images of the plant from a great distance, resulting in insufficient resolution to identify individual plant organs. Here, feature extraction mostly relies on estimating the proportions of different coloured pixels, without shape information. This data is expected to have more noise, for example due to changing lighting conditions during a measurement. For example Zhang et al. and Marzougui et al. examined the flower intensity of crops utilizing UAV and diverse sensor techniques in outdoor conditions [7, 15]. However, pixel-based approaches can lead to lower accuracy during main flowering, since it single flowers are not distinguishable when taking images from too far away [7]. In contrast, ground-based HTFP methods for flowering have mostly been focusing on single plants, as for example Yoon et al., who have detected the receptacles of strawberries or Jiang et al. who focused on flowering of cotton [6, 16]. However, regular field crops are sown in dense stands, where the proposed approaches are not applicable.

We combined the advantages of ground based HTFP and newest development in imaging analysis, by using a deep learning approach with Convolutional Neural Networks (CNN). Images of various pea breeding lines in field conditions were collected with the Field Phenotyping Platform (FIP), a stationary platform of ETH Zurich [17]. For flower detection, we trained a deep learning approach with object detection. The objectives of our study were to i) develop an image-based approach to investigate flower intensity and pods in RGB images; ii) to evaluate the accuracy of the results; and iii) to compare the results to manually rated data and yield components in different breeding lines.

2 Methods

2.1 Experimental Design and Plant Material

We conducted field experiments in 2022 and 2023 with 12 leafless pea breeding lines, which were selected for variety testing. The experiment took place at the Plant Research Station of ETH Zurich, in Eschikon, Switzerland (47.449 N, 8.682E, 520 m a.s.l.). Soil properties were previously described

as gleyic cambisol [17]. The breeding lines were sown in 1.5 m x 6 m plots with nine rows and a seed density of 80 seeds per square-meter. In both years, the experimental design was a randomised complete block design (RCBD) with three replications, resulting in 36 experimental plots per year. In 2022, the peas were sown on 10-03-2022 and harvested on 07-07-2022. In 2023, the peas were sown on 17-03-2023 and harvested on 14-07-2023. The following varieties were used: Astronaute, Avatar, Greenway, Kagnotte, Kameleon, Kazek, Orchestra, Paprika, and Torpedo, which are listed in the European variety catalogue [18]. Additionally, Belcon_10_9_6_2, Conpro_10_3_2_8, Sallam_10_8_7_1 were used, which were bred by the local breeders of Getreidezüchtung Peter Kunz (GZPK), Hombrechtikon, Switzerland.

2.2 Post-harvest processing of seeds

The protein and water content of the dried peas were determined using Near Infrared Reflectance Spectroscopy (NIRS, version IM 9500, Perten Instruments NA, Inc., Springfield, U.S.A., calibrated for peas). Thousand Kernel Weight (TKW) was determined with MARViN ProLine II seed analyzer from MARViTECH GmbH (Wittenburg, Germany). The yield data was corrected with the water content of the corresponding plot values and calculated to dry matter (DM).

2.3 Image Acquisition

During the whole flowering phase of the pea plants, we acquired images twice a week resulting in ten data collection days (six in 2022 and four in 2023), as it can be seen in Figure 1. In addition, we also took images from two to three days before the peas were harvested to investigate number of pods.

Images were collected by using the FIP [17]. The FIP is a rope suspended carrier system that holds multiple sensors, including RGB cameras. This allows to take images from plants with an approximately distance of 2.5 m. Images in 2022 were made by a 21 MP full frame DSLR camera, model: EOS 5D Mark II (Canon Inc., Tokyo, Japan). Images in 2023 were made by a 12.3 MP camera (The Imaging source, Germany) carrying a Sony CMOS Pregius IMX 304 Sensor, model: DFK 38UX304. The camera used in 2022 delivered a ground sampling distance of $\sim$0.3 mm, while the camera from 2023 a ground sampling distance of $\sim$0.9 mm. In both years, images were taken from approximately 2.5 m above canopy in nadir view.

2.4 Ground truth and field data

In order to gather ground truth data for open flowers and ripe pods, we counted objects of interest in the field and on images. In a first step, we manually counted open flowers and pods in the field in a Region of Interest (ROI) in 24 plots in 2023. The ROI, sized at 50 x 50 cm, was marked out using wooden sticks with blue heads (S.3A) and all open flowers and ripe pods within this area were counted manually. The counting in the field took place in the same hour that the FIP-images were taken. In a second step, we counted the flowers and pods in the ROI on the FIP images manually (S.3C) in the Computer Vision Annotation Tool (CVAT) [19]. Ground truth for flowers were counted

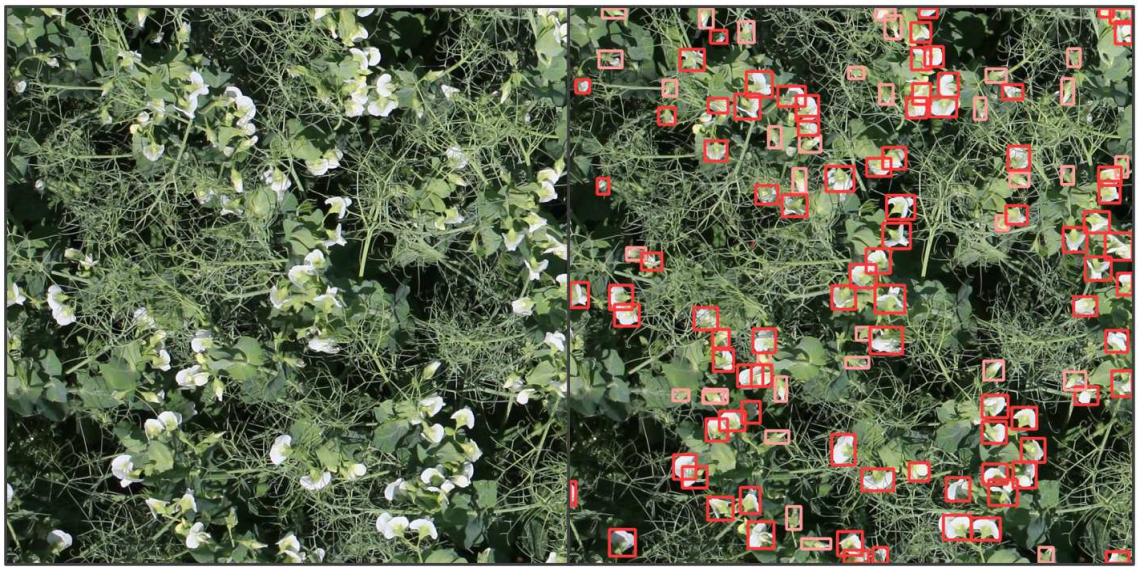

Figure 1: Visualisation of the open pea flowers detected by the object detection model. Left: Part of an FIP image with pea flowers. Right: red boxes show pea flowers detected by the model.

on all measurement days in 2023 while pods were counted once. In addition, BBCH-growth stage was rated at plot-level manually, at the same days the images were taken. Lodging, who has an affect on visibility of plant organs, was rated visually once, where no lodging received a zero and lodging received a one. All field data was collected by using the "Field Book App" [20].

2.5 Trait extraction

To detect pea flowers on RGB-Images we used an efficient YOLOv8m detection model [21]. YOLOv8 is a fully convolutional deep learning model which we utilized for object detection. YOLOv8 has also recently been used by Jiang et al., to investigate pea seeds during germination [22]. In contrast to its predecessor YOLOv5 [23] it uses an anchorless approach for object detection. This enabled us to train a model on small image patches and then scale the model to large, uncropped images without compromising the performance.

We manually labelled bounding boxes around pea flowers and pods in a training set of 371 1024x1024px image patches from 2022. This consisted of 287 randomly selected images containing mainly flowers and 84 randomly selected images containing mainly pods. Image annotation with bounding boxes was done in the open-source CVAT [19]. We labelled four classes: open_flowers, other_flowers, ripe_pods and green_pods. For labelling, open pea flowers were defined by their shape (clearly recognisable semicircular) and clear white coloration, while other flowers are identifiable as flowers but not open. Ripe pods were also defined by their color (brown) and shape (as shown in Figure S.2), while green pods are defined by pod shape and green color.

The model was trained on the full resolution with a default selection of augmentations to make it more robust against different lighting conditions and/or images from other sensors. This included augmentations of blurring, contrast and grey scale. The model was trained with 50 epochs and a batch size of four. The model training was performed using a stochastic gradient descent (SDG) with a initial learning rate of 0.01. The training and validation split was 4:1. For prediction, the trained model was used on FIP-images from 2022 and 2023 to detect flowers and pods with a confidence of 0.31. Images taken by the FIP tend to show more than solely the experimental plot. Therefore, plots were manually cropped from the images what resulted in slightly different image sizes. Images to predict were resized to 2700x5500px for 2022 and 1300x4000px for 2023. Flower counts were conducted at the plot level and then converted to flowers per square meter based on plot size.
To evaluate the model performance, the F1-score was evaluated. The F1-score calculates the harmonic mean of precision and recall. Also the results were compared to the collected ground truth data.

2.6 Statistical Analysis

To compare data of two years, dates are always displayed in Days After Sowing (DAS). The BBCH-stages that were investigated were determined as follows during rating in the field: 61: Start of Flowering (10% of plants carry an open flower); 65: Flowering (50% of plants carry an open flower); 69: End of Flowering. Loess-regression was used to fit values of open flowers or BBCH-stages on days when no measurement were taken. To reduce the effect of field heterogenity, the values were spatially corrected by using the "SpATS Package" in RStudio [24]. With this, two-dimensional penalised splines (P-splines) are used, which allows to extract the best linear unbiased estimation values (BLUE). This gives a combined, predicted value for each breeding line, which will be referred to as "spatially corrected". This also allows to provide heritability (h^2) of traits.

2.7 Maximal number of open flowers and fruiting efficiency

With the model provided numbers of open flowers two main variables were calculated: Maximal number of open flowers (Max.Flowers.No), which display the maximal number of open flowers per m^2. And day when maximal number of open flowers is reached (Max.Flowers.DAS), which represents the day after sowing. To investigate Max.Flowers.No together with TKW as an estimate for yield in each year, we used the following linear model:

$$Yield_{ij} = TKW_{ij} + Max.Flowers.No_{ij} + Year_j + \varepsilon_{ij} \quad (1)$$

where yield ($Yield_{ij}$) of the i^{th} breeding line in the j^{th} year was modelled with a fixed effect for TKW (TKW_{ij}), Max.Flowers ($Max.Flowers.No_{ij}$) and an associated error (ε_{ij}) with $\varepsilon \sim N(0, I\sigma^2_\varepsilon)$. Logarithmic transformed values were used for Yield and Maximal amount of flowers.

Max.Flowers.No was also used to calculate fruiting efficiency which we defined as the ratio of Max.Flowers.No and harvested seeds per square-meter.

3 Results

Field experiments were conducted in two field seasons with 12 pea breeding lines. Images were taken twice a week during the flowering period, which was in six measurements during 2022 and four in 2023, resulting in 216 and 144 images respectively. For data evaluation, the accuracy of the object detection model was analysed first. Subsequently, flowering dynamics of all breeding lines were extracted and yield components such as protein content and grain yield were analysed finally.

3.1 Accuracy of the model

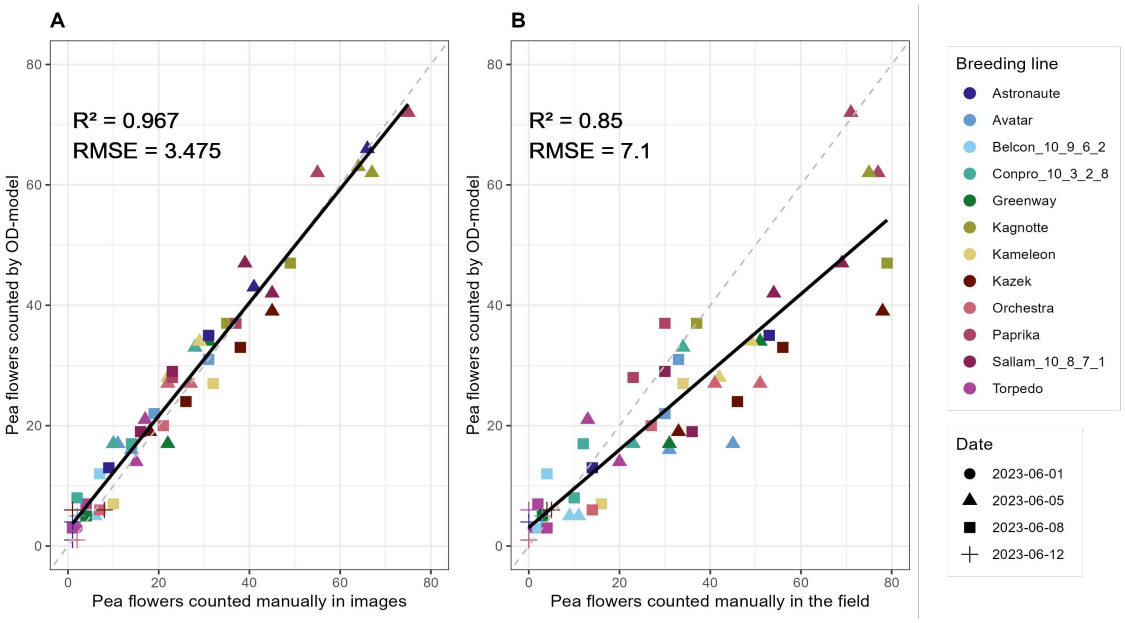

Figure 2: Accuracy of the object detection model for open flowers. Detected flowers compared to ground truth values from 2023. A: Manually counted open flowers in images versus open flowers counted by the object detection model. Linear Equation: y = 0.941x + 2.782. B: manually counted open flowers in the field versus open flowers counted by the object detection model; Colors indicate different breeding lines (n=12) and shapes indicate different dates (n=4). Black line indicates the linear regression line. Grey dashed line indicates 1:1 - correlation.

The trained model achieved an F_1-score of 0.82 for open flowers and 0.76 for ripe pods. The mean average precision (mAP50) for open flowers was 0.88 and for ripe pods 0.80 1. Open flowers and ripe pods have higher values when compared to their counterpart (other flowers, green pods; Figure S.1). For this reason, and because they are the most important yield parameters, we decided to focus only on open flowers and ripe pods. Therefore, we refer to open flowers as "flowers" and mature pods as "pods" unless otherwise noted.

The number of manually counted flowers on images and the number of flowers counted by the model was highly correlated (R^2= 0.967, Figure S.3A). Nonetheless, when numbers of flowers counted

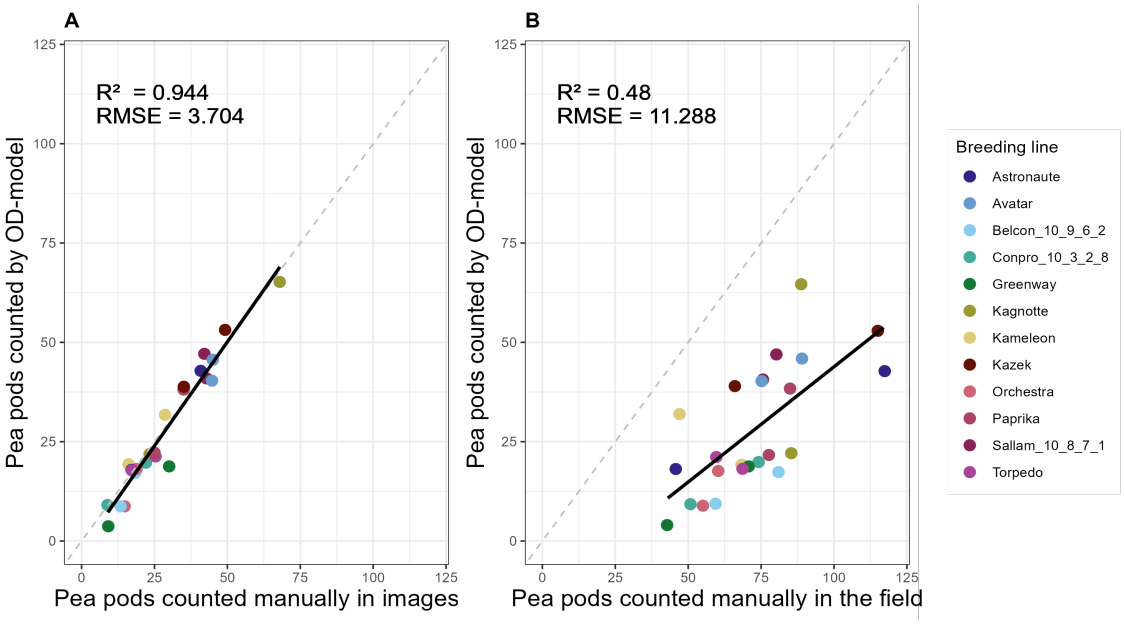

Figure 3: Accuracy of the object detection model for ripe pods. Detected pods compared to ground truth values from 2023. A: Manually counted ripe pods in image versus ripe pods counted by the object detection model. Linear equation: y= 1.047x + -2.237. B: manually counted ripe pods in the field versus ripe pods counted by the object detection model; Black line indicates the linear regression line. Grey dashed line indicates 1:1 - correlation. Ripe pods were counted on the 04-07-2023.

by the model are compared to flowers counted manually in the field, less flowers were detected by the model (R^2=0.85; Figure2B). The Root Mean Squared Error (RMSE) was two times higher for the comparison between model detected values and manually counted in the field than compared to manually counted in images. The differences between the flowers detected by the model and flowers counted in the field seemed not specific for any breeding line or date.

Similar as for the open flowers, the results for pods detected by the model and pods visible in the images are highly correlated (R^2=0.9444, RMSE=3.704) as visible in Figure 3A. However, correlation between pods detected by the model and pods counted in the field is lower compared to results obtained for flowers (R^2=0.48, RMSE=11.288, Linear equation: y= 0.58x + -14.164) as shown in Figure 3B.

3.2 Flower intensity and dynamics in different breeding lines

Trait	h^2
TKW [g]	0.97
Seeds [m^2]	0.93
Pods [m^2]	0.82
Protein [%]	0.67
Yield [t/ha]	0.85
BBCH 65	0.87
BBCH 69	0.89
Max.Flowers.No	0.78
Max.Flowers.DAS	0.85

Table 1: Broad-sense heritability (h^2) of the traits over two years using spatial correction.

The twelve breeding lines showed different dynamics of flower onset and/or intensity over time (Figure 4). In 2022, the Max.Flowers.No ranged from 30 per m^2 in Belcon_10_9_6_2 to 95 per m^2 in Paprika. In 2023, the range was between 3 per m^2 in Kazek and 14 per m^2 in Kagnotte, according to the fitted values. It was clearly visible, that in 2022 more flowers were open on a day for each breeding line than in 2023. The flowering period of the pea plants took place over 20 days in 2022, while in 2023 flowering lasted for about 14 days, as seen in Figure 4.

The heritability (h^2) of the flowering traits provided by the model (Max.Flowers.No, Max.Flowers.DAS) were high with 0.78 and 0.85, respectively (Table 1). The growth stage related manually rated traits, were higher with heritability of 0.87 for BBCH 69 (end of flowering) and 0.89 for BBCH 65 (main flowering). The comparison to the manual rated BBCH stages (Figure 4, vertical lines) showed that the start of flowering (BBCH 61; "10% of plants carry an open flower") fits well in the first third of open flowers occurring. The "flowering timepoint" or BBCH 65, was determined by visual ratings generally before the Max.Flowers.No was reached.

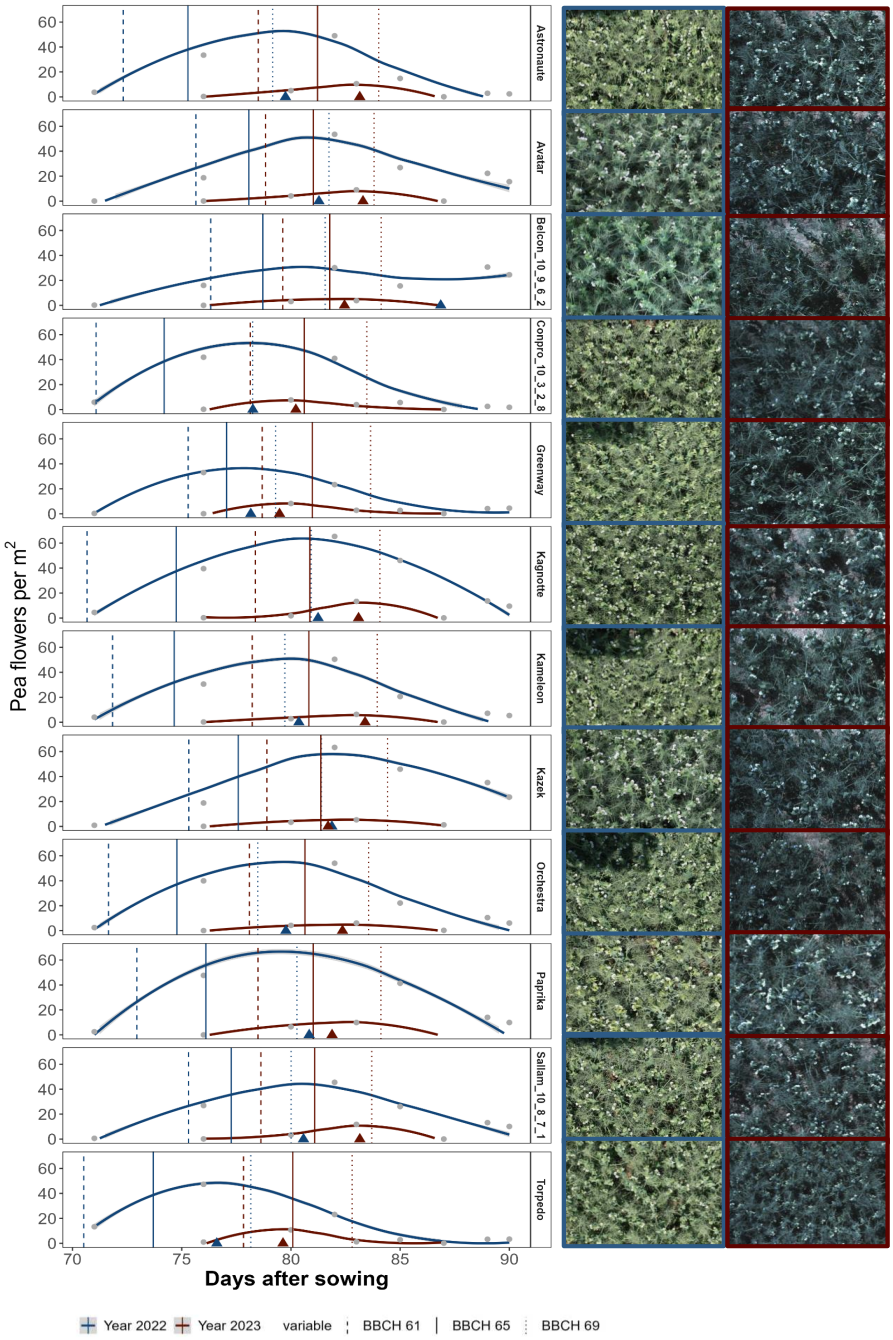

Figure 4: Overview of the flowering dynamics of twelve different pea breeding lines. Left: The evolution of flower intensity of the different breeding lines over time in days after sowing, data from 2022 (blue) and 2023 (red). The grey points indicate measured values (spatially corrected); the lines indicate Loess- fitted values for each breeding line. Vertical lines display manually rated BBCH stages (spatially corrected) for comparison. Triangles indicate Max.Flowers.DAS Right: Section of each breeding line is depicted on day of Max.Flowers.No.

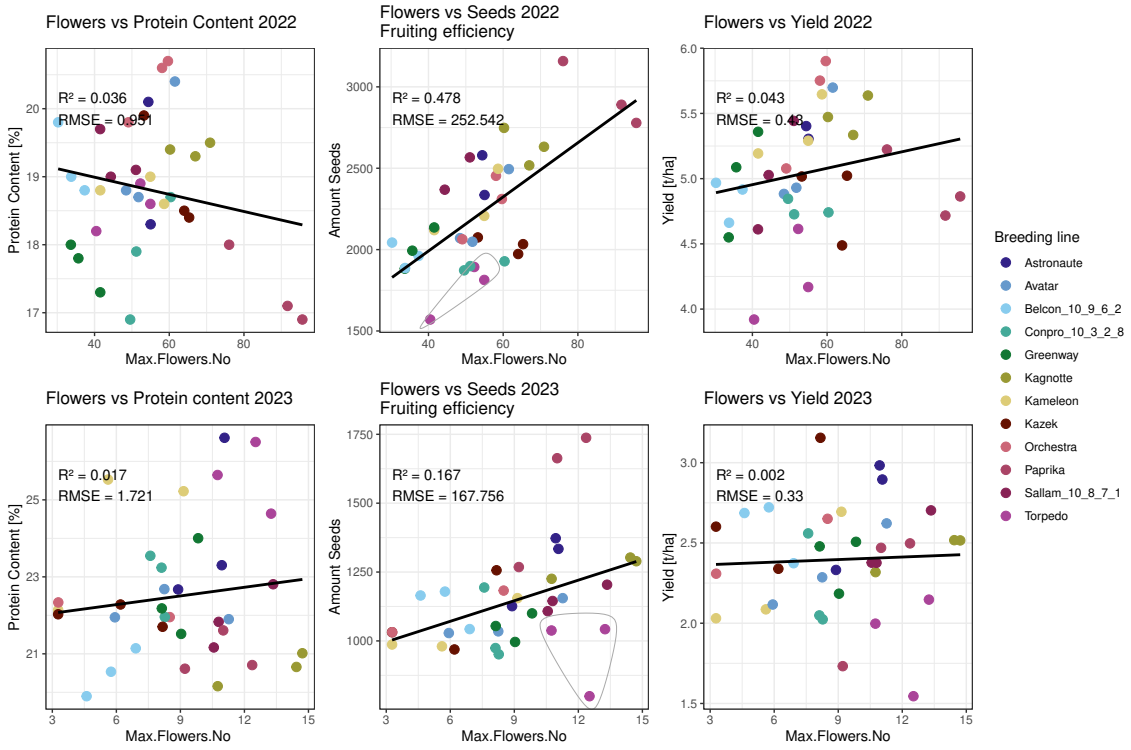

Figure 5: Correlation between the Max.Flowers.No and yield, protein content and amount of seeds (Top: 2022 values; bottom: 2023 values). Different colours indicate 12 breeding lines in three replications (n=36) on plot level.

3.3 Yield data and fruiting efficiency

Grain yield was higher in 2022 than 2023, while protein content was slightly higher in 2023 (Figure S.5). For protein content and yield there were slight positive and negative correlation in 2022 and 2023, respectively. However, comparing the Max.Flowers.No with seed amount, which results in fruiting efficiency, showed in both year a positive correlation, in 2022 a with a R^2-value of 0.478 and in 2023 a R^2-value of 0.167 (Figure 5). The breeding line Torpedo exhibited outlier-like values in 2023 due to its high Max.Flowers.No but low number of seeds at the end (Figure 5 grey line).

The variance of yield explained by Max.Flowers.No and TKW for yield, was calculated by the linear model (Equation 1). This resulted in a multiple R^2 of 0.919, while the year had the highest influence (Table 2).

3.4 Correlation of traits

Model provided traits, such as Max.Flowers.No and Max.Flowers.DAS, showed high correlation with yield components, as shown in Figure 6. Max.Flowers.DAS was highly correlated with BBCH 65 with 0.6 and even higher with BBCH 69 with 0.84. Max.Flowers.DAS showed also correlation with 0.59 with pods per m^2. Max.Flowers.DAS had a high correlation with seeds per m^2 with 0.77 and

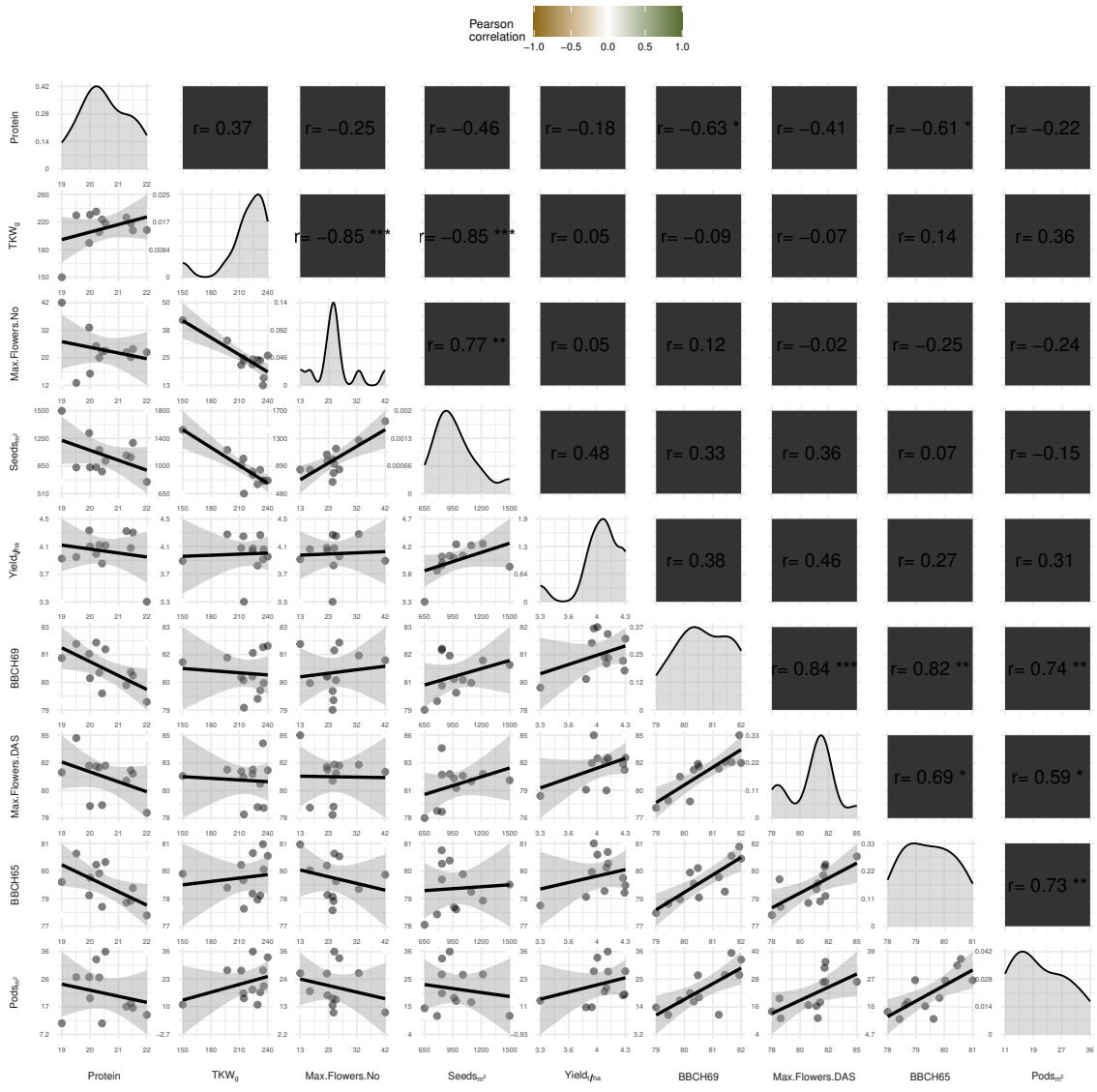

Figure 6: Correlation plot (Pearson correlation) between various variables in both years with spatially corrected values. Darker values indicate higher correlation, where green are positive and yellow are negative correlation. Significance is shown with stars, where *p<0.05; **p<0.01; ***p<0.01

Variable	Estimate	Std. Error	t value	Pr($>\|t\|$)
TKW	1.829e-03	6.378e-04	2.868	0.00554
Max.Flowers.No	1.027e-01	4.746e-02	2.164	0.03408
Year	-5.286e-01	9.717e-02	-5.440	8.38e-07
Statistic	**Value**			
Residual standard error	0.1157			
Multiple R-squared	0.9186			
Adjusted R-squared	0.9149			
F-statistic	248.2			
Degrees of freedom (DF)	3 and 66			

Table 2: Linear Regression Results

even higher with TKW (-0.85). The correlation between BBCH 65 and BBCH 69 was high (0.82). It should be noted that these variables are interdependent and therefore result in high correlation. However, the BBCH 65 and BBCH 69 also showed a high correlation with pods per m^2 at 0.73 and 0.74 respectively.

However, the correlation between the variables has differed in the two years, as visible supplementary Figures S.6 and S.7.

4 Discussion

The results showed positive correlations between yield components, such as amount of seeds, pods and the Max.Flowers.No. The observed flowering dynamics were similar to the growth stages identified through manual ratings. Therefore, the described HTFP method has potential to replace manual ratings while delivering more detailed phenotypic information, e.g. about flower intensity or fruiting efficiency.

4.1 Accuracy of the Object Detection Model

The model achieved a solid performance resulting in a higher F1-score for open flowers compared to that for ripe pods. The slightly lower performance on the task of detecting pods is probably due to fewer pods instances in the dataset and generally less distinct visual features of the pods compared to flowers and the rest of the canopy.

The object detection model provided numbers of open flowers with high accuracy (R^2 =0.967), when compared to numbers of flowers from manual counting on images. This accuracy is comparable or even better when compared to previously published studies of object detection models recognising plant organs, e.g. [6, 7, 25]. This demonstrates, eventhough the images were taken with a different camera than the images the model was trained on, the results are still reliable. Hence, that the proposed image based determination of flowering stages could probably be performed on images with high resolution smartphone cameras. This provides an opportunity for the practical application of

this approach.

The model also provided high accuracy for the detected pods. Comparing the two ground truth datasets (Figure 2 and 3) provides interesting insights into the structure of pea yield components. While the flowers are well visible in the images taken from above, the pods are not. This is due to the fact that the pea plant bears its flowers at the top, leading to pod formation. Also, the RMSE was lower for comparison of model detected values (flowers and pods) compared to manually counted on images than manually counted in the field. Meaning that there are probably even more flowers or pods not captured in the images. Nonetheless, also in manual ratings done by evaluators in the field, occlusions can hinder a precise assessment of flower intensity. Thus, the next performance leap will not be achieved by improving the object detection model but rather the imaging methodology. For further insights in the number and flowering structure or pods from pea plants, an approach with multiview images would be helpful, as it was done in various studies, i.e. [14, 26]. Multiview images can infer geometric structure and reconstruct 3D images when multiple cameras capture images from different angles [27].

4.2 Flower intensity and dynamics in different breeding lines

Compared to manually rated values, the model detected numbers of flowers, that allowed to display flower dynamics, were well in line with growth stage ratings (BBCH stages). The Max.Flowers.DAS had a comparable heritability, as shown in table 1. This showed that the model-detected values allow to monitor flower dynamics in a comparable way as manual ratings, which could replace manual ratings. In previous studies where flowering was monitored with UAV, a decreased accuracy during maximal bloom was observed [7]. Yet, this was not observed in our study, since the comparsion of detected open flowers to ground truth data showed that in our study, the accuracy was not lower during main flowering.

4.3 Yield and protein content

There were clearly visible year effects especially in Max.Flowers.DAS, flowering period length, and grain yield, likely due to the differences in temperature and precipitation. In 2023, almost no precipitation was recorded before and during flowering (Supplementary Figure S.4). Contrasting to grain yield, the protein contentwas higher in 2023 than in 2022. According to the literature, there is a correlation between temperature and precipitation to the protein content of summer peas [28–30]. Nevertheless, the higher protein content in 2023 can be explained by the fact that protein content is negatively correlated with yield [31]. Bueckert et al. [32] stated that drought and heat tolerance from peas could be addressed by breeding to earlier start of flowering, which also stresses the importance of flowering as a trait in breeding.

4.4 Relation of open flowers and seeds and fruiting efficiency

Interestingly, breeding lines with a higher Max.Flowers.No tended to have more seeds with lower TKW(Figure 6). This although the number of observed flowers over the season may not be additive, i.e., the total number of flowers is unknown. Notably, the environmental influences may affect the rate of pod or flower abortion. In 2023, where almost no precipitation was recorded around flowering, the flower intensity was significantly lower than in 2022. This is aligning with the literature, as drought or heat stress during flowering can lead to a higher rate of flower and pod abortion [33, 34] while precipitation has led to longer reproductive growth and higher yield [32]. According to the literature, especially the early reproductive phase has been identified to be sensitive to heat stress. Osorio et al. [34] have recently shown that various post-fertilization events are disturbed by high temperature. Heat and/or drought stress are major drivers for flower or pod abortion, and eventually yield loss [11]. For example, as seen in figure 5, the breeding line Torpedo has had a high number of open flowers per day and resulted in a smaller number of seeds, when compared to others, which could be described as lower fruiting efficiency. Also the grain yield of Torpedo was smaller compared to the other breeding lines (Supplementary Figure S.5). These observations may show that Torpedo has a lower tolerance to heat or drought stress during reproductive phase, as drought was a stress factor in 2023. Here, the model provided number of open flowers show a clear advantage compared to manual ratings. It would not have been possible to count numbers of open flowers manually for each plot twice a week, and therefore also not possible to calculate a reliable fruiting efficiency. By observing the number of open flowers from a breeding line, the fruiting efficiency can be introduced in breeding for more heat and/or drought tolerant breeding lines. Breeding towards heat and/or drought tolerant lines was also proposed by Bueckert et al. [32]. However, until now, breeding for higher fruiting efficiency (ratio of reproductive organs / seeds) has lacked reliable data, which can be obtained with the proposed method.
Further research is required to observe individual flowers over time. This could also be addressed by using the proposed model, as YOLO-based object detection models, can not only detect objects but also localise them [26]. Another improvement would be the use of multiview images which could bring more insight in flowering structure, e.g. as done in Jiang et al. [6].

Maximal flower intensity (Max.Flowers.No) in combination with TKW explains over 90% of the variance for yield, according to the linear model (Equation 1). TKW is a highly heritable trait (h^2=0.97) while Max.Flowers.No is more determined by environmental factors (h^2=0.78). Therefore, Max.Flowers.No should be investigated in more environments to make it a reliable predictor for yield. The proposed methods offers great potential for automated data collection about Max.Flowers.No in various environments.

4.5 Pods

There was a positive and significant correlation between the Max.Flowers.No and the number of seeds per m^2 . The quantity of seeds not only affected the final grain yield but also served as an indicator for investigating flower and pod abortion. Nevertheless, the occurred lodging of plants in

2022, does not allow to make precise predictions about the relation between flowers and pods per m^2. As seen in Supplementary Figure S.7, the numbers of pods per m^2 in 2023 only had a high correlation with Max.Flowers.DAS. Compared to this, in 2022 the correlation is much higher (see Supplemental Figure S.7). This is explainable by the issue that pods were not well visible from above, but from the side - which is only possible when the plants were lodging. However, as seen in Figure 3, the detected number of pods from images, taken from above, compared to the ground truth does not provide too much insights into the number of pods per m^2. For further investigation of pods per m^2, a multiview approach would be needed.

5 Conclusion

The presented method, a combination of automatic collected RGB-images and an object detection model, demonstrates the use of image based methods for monitoring flower intensity and dynamics of various pea breeding lines. The resulted heritabilities of the model based traits were comparable to manual ratings, which makes this approach a promising alternative to manual ratings in the field. To improve pea flower detection and avoid occlusions by other plant organs, the approach could be even further developed with multiview images. In addition, by using common RGB-images, this method has shown potential for practical approaches, such as implementing with smartphones. Since detecting pea flowers also allows to predict seed amount as an important yield component or to calculate fruiting efficiency with HTFP, this method could support selection decisions. The potential of the model to detect not only flowers but also pods opens possibilities to address physiological questions such as the flower or pod abortion.

Acknowledgments

We sincerely thank Simon Corrado for managing and nursing the field experiments perfectly, and all the FIP-operators of the Crop Science Group, namely Norbert Kirchgessner, Flavian Tschurr and Olivia Zumsteg. We further thank DSP (Delley Samen und Pflanzen AG) and GZPK (Getreidezüchtung Peter Kunz) for providing the seeds for the conducted experiments. Special thanks to Mirjam Chassot for annotating the training data and to Michelle Kremers and Isabelle Reichlin for supporting the data collection in field experiments.

Declarations

Author Contributions

C. Oppliger: Conceptualisation, methodology, formal analysis, visualisation, data acquisition, writing - original draft; B. Keller: Supervision, methodology, formal analysis, visualisation, data acquisition, writing— review and editing; R. Zenkl: Software, writing - review and editing; A. Walter: Supervision, project administration, writing— review and editing.

Conflicts of Interest

The authors declare that there is no conflict of interest regarding the publication of this article.

Data Availability

Code will be available on gitlab.ethz and data will get a separate doi after acception.

Ethical Approval

Not applicable.

Funding

Open access funding provided by Swiss Federal Institute of Technology Zurich.

References

1. Hall C, Hillen C, and Garden Robinson J. Composition, Nutritional Value, and Health Benefits of Pulses. Cereal Chemistry Journal 2017;94:11–31.
2. Mathesius U. Are legumes different? Origins and consequences of evolving nitrogen fixing symbioses. Journal of Plant Physiology 2022;276:153765.
3. Steinfeld H. Livestocks Long Shadow. Rome: FOOD AND AGRICULTURE ORGANIZATION OF THE UNITED NATIONS, 2006.
4. Semba RD, Ramsing R, Rahman N, Kraemer K, and Bloem MW. Legumes as a sustainable source of protein in human diets. Global Food Security 2021;28:100520.
5. Harwatt H, Sabaté J, Eshel G, Soret S, and Ripple W. Substituting beans for beef as a contribution toward US climate change targets. Climatic Change 2017;143:261–70.
6. Jiang Y, Li C, Xu R, Sun S, Robertson JS, and Paterson AH. DeepFlower: a deep learning-based approach to characterize flowering patterns of cotton plants in the field. Plant Methods 2020;16:156.
7. Zhang C, Craine W, McGee R, et al. Image-Based Phenotyping of Flowering Intensity in Cool-Season Crops. Sensors 2020;20:1450.
8. Möller-Steinbach Y, Alexandre C, and Hennig L. Flowering Time Control. In: *Plant Developmental Biology*. Ed. by Hennig L and Köhler C. Vol. 655. Series Title: Methods in Molecular Biology. Totowa, NJ: Humana Press, 2010:229–37. DOI: 10.1007/978-1-60761-765-5_15. URL: http://link.springer.com/10.1007/978-1-60761-765-5_15 (visited on 11/14/2022).
9. Turner NC, Davies S, Plummer J, and Siddique K. Seed Filling in Grain Legumes Under Water Deficits, with Emphasis on Chickpeas. In: *Advances in Agronomy*. Vol. 87. Elsevier, 2005:211–50. DOI: 10.1016/S0065-2113(05)87005-1. URL: https://linkinghub.elsevier.com/retrieve/pii/S0065211305870051 (visited on 05/31/2022).

10. Weller JL and Ortega R. Genetic control of flowering time in legumes. Frontiers in Plant Science 2015;6.

11. Mohapatra C, Chand R, Tiwari JK, and Singh AK. Effect of heat stress during flowering and pod formation in pea (Pisum sativum L.) Physiology and Molecular Biology of Plants 2020;26:1119–25.

12. Gogoi N, Farooq M, Barthakur S, et al. Thermal Stress Impacts on Reproductive Development and Grain Yield in Grain Legumes. Journal of Plant Biology 2018;61:265–91.

13. Fang X, Turner NC, Yan G, Li F, and Siddique KHM. Flower numbers, pod production, pollen viability, and pistil function are reduced and flower and pod abortion increased in chickpea (Cicer arietinum L.) under terminal drought. Journal of Experimental Botany 2010;61:335–45.

14. Das Choudhury S, Guha S, Das A, Das AK, Samal A, and Awada T. FlowerPhenoNet: Automated Flower Detection from Multi-View Image Sequences Using Deep Neural Networks for Temporal Plant Phenotyping Analysis. Remote Sensing 2022;14:6252.

15. Marzougui A, McGee RJ, Van Vleet S, and Sankaran S. Remote sensing for field pea yield estimation: A study of multi-scale data fusion approaches in phenomics. Frontiers in Plant Science 2023;14:1111575.

16. Yoon S, Jo JS, Kim SB, Sim HS, Kim SK, and Kim DS. Prediction of strawberry yield based on receptacle detection and Bayesian inference. Heliyon 2023;9:e14546.

17. Kirchgessner N, Liebisch F, Yu K, et al. The ETH field phenotyping platform FIP: a cable-suspended multi-sensor system. Functional Plant Biology 2017;44:154.

18. Johan B. Common catalogue of varieties of agricultural plant species. 2023.

19. Sekachev B, Manovich N, Zhiltsov M, et al. opencv/cvat: v1.1.0. Version v1.1.0. 2020. DOI: 10.5281/ZENODO.4009388. URL: https://zenodo.org/record/4009388 (visited on 03/06/2023).

20. Rife TW and Poland JA. Field Book: An Open-Source Application for Field Data Collection on Android. Crop Science 2014;54:1624–7.

21. Jocher G, Chaurasia A, and Qiu J. YOLO by Ultralytics. Version 8.0.0. 2023. URL: https://github.com/ultralytics/ultralytics.

22. Jiang H, Hu F, Fu X, et al. YOLOv8-Peas: a lightweight drought tolerance method for peas based on seed germination vigor. Frontiers in Plant Science 2023;14.

23. Jocher G, Chaurasia A, Stoken A, et al. ultralytics/yolov5: v7.0 - YOLOv5 SOTA Realtime Instance Segmentation. Version v7.0. 2022. DOI: 10.5281/ZENODO.3908559. URL: https://zenodo.org/record/3908559 (visited on 11/28/2023).

24. Rodríguez-Álvarez MX, Boer MP, Eeuwijk FA van, and Eilers PH. Correcting for spatial heterogeneity in plant breeding experiments with P-splines. Spatial Statistics 2018;23:52–71.

25. Stein M, Bargoti S, and Underwood J. Image Based Mango Fruit Detection, Localisation and Yield Estimation Using Multiple View Geometry. Sensors 2016;16:1915.

26. Jiang Y and Li C. Convolutional Neural Networks for Image-Based High-Throughput Plant Phenotyping: A Review. Plant Phenomics 2020;2020:2020/4152816.

27. Roth L, Camenzind M, Aasen H, et al. Repeated Multiview Imaging for Estimating Seedling Tiller Counts of Wheat Genotypes Using Drones. Plant Phenomics 2020;2020:2020/3729715.

28. Walter S, Zehring J, Mink K, Quendt U, Zocher K, and Rohn S. Protein content of peas (Pisum sativum) and beans (Vicia faba)—Influence of cultivation conditions. Journal of Food Composition and Analysis 2022;105:104257.

29. Lizarazo CI, Lampi AM, Liu J, Sontag-Strohm T, Piironen V, and Stoddard FL. Nutritive quality and protein production from grain legumes in a boreal climate: Production of grain legumes in a boreal climate. Journal of the Science of Food and Agriculture 2015;95:2053–64.

30. Nikolopoulou D, Grigorakis K, Stasini M, Alexis M, and Iliadis K. Differences in chemical composition of field pea (Pisum sativum) cultivars: Effects of cultivation area and year. Food Chemistry 2007;103:847–52.

31. Patil G, Mian R, Vuong T, et al. Molecular mapping and genomics of soybean seed protein: a review and perspective for the future. Theoretical and Applied Genetics 2017;130:1975–91.

32. Bueckert RA, Wagenhoffer S, Hnatowich G, and Warkentin TD. Effect of heat and precipitation on pea yield and reproductive performance in the field. Canadian Journal of Plant Science 2015;95. Publisher: NRC Research Press:629–39.

33. Guilioni L. Heat Stress-induced Abortion of Buds and Flowers in Pea: Is Sensitivity Linked to Organ Age or to Relations between Reproductive Organs? Annals of Botany 1997;80:159–68.

34. Osorio E, Davis AR, Warkentin TD, and Bueckert RA. Ovule abortion and seed set of field pea (*Pisum sativum* L.) grown under high temperature. Canadian Journal of Plant Science 2023;103:270–84.

Supplementary Materials

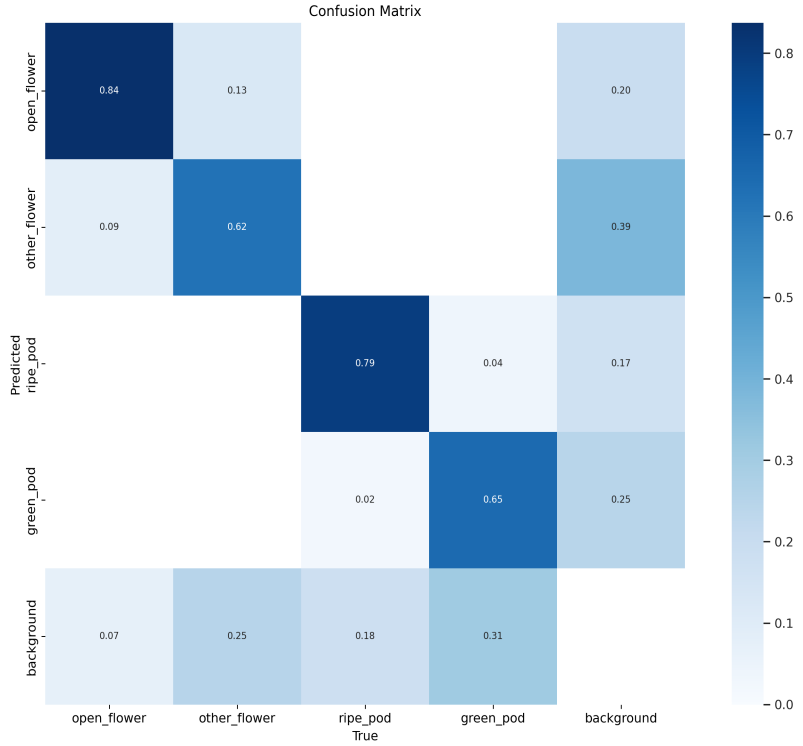

Figure S.1. Confusion matrix of object detection model for pea organs, comparing the predicted and true values. Darker colors indicate higher recall values.

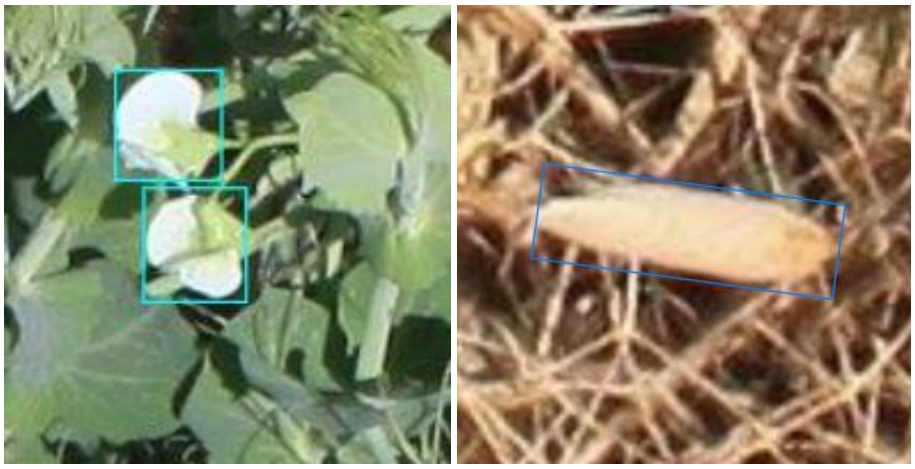

Figure S.2. Example of how annotations were made. Turquoise box: open pea flower. Blue: ripe pea pod.

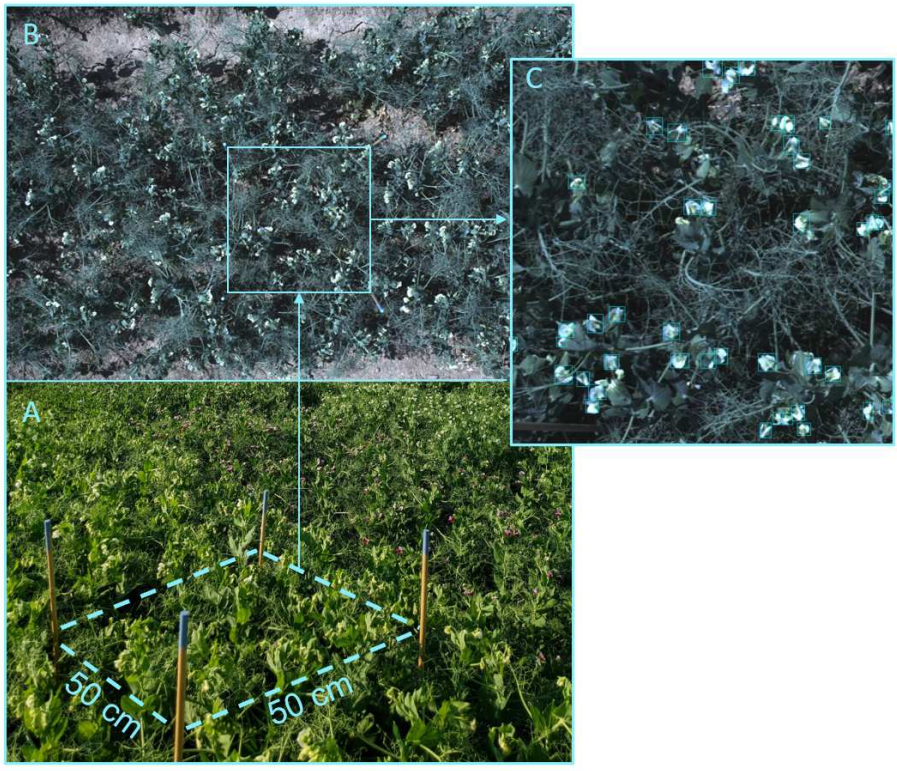

Figure S.3. Overview of the ground truth data collection. A: Region of interest (ROI) in the field, determined by the wooden sticks with a blue head, 50 x 50 cm. In this area the flowers were counted manually. B: FIP-Image of a plot, well visible the ROI,due to the blue heads of the wooden sticks. C:flower counting in images in the ROI was done by the model and manually.

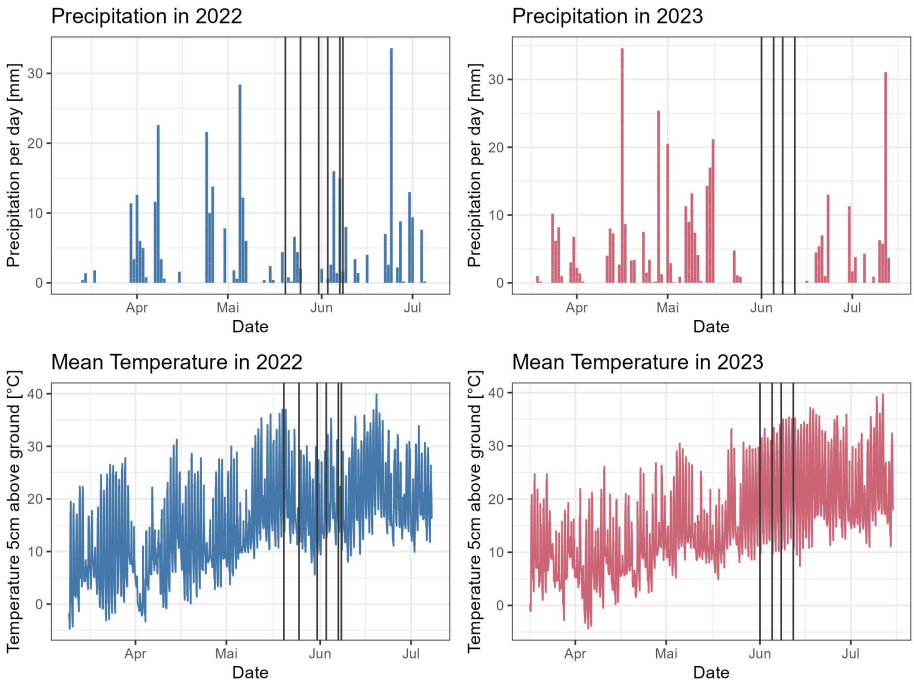

Figure S.4. Weather data (temperature and precipitation) during the field experiments. Data from agrometeo.ch. Blue figures for 2022 and red figures for 2023. Grey lines indicate measuring time points and therefore flowering period. Total precipitation was 347mm in 2022 and 381mm in 2023.

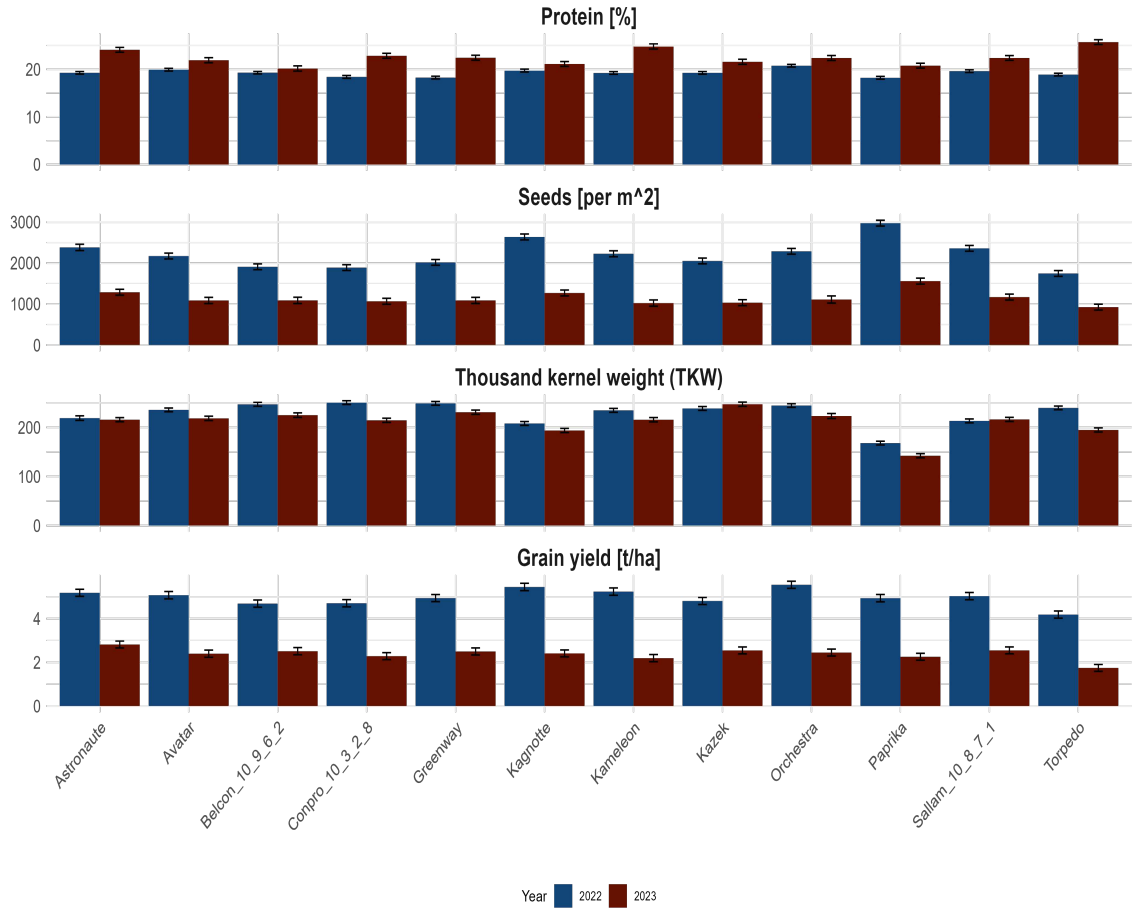

Figure S.5. Yield data from the different breeding lines from 2022 (blue) and 2023 (red). The values are spatially corrected and shown with standard error.

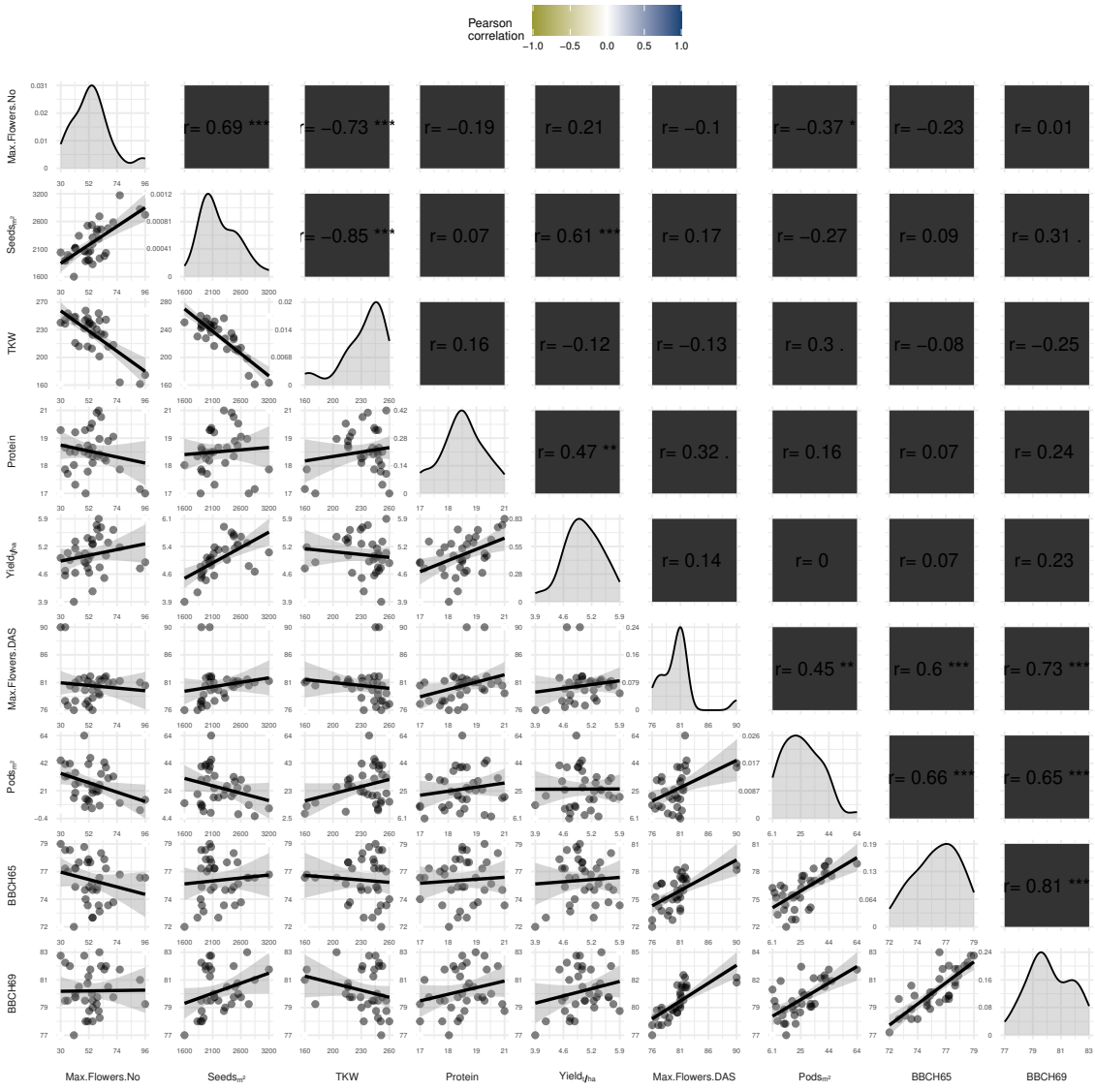

Figure S.6. Correlation plot of all variables on plot level from Year 2022. Darker values indicate higher correlations. Significance is shown with stars, where *p<0.05; **p<0.01; ***p<0.01

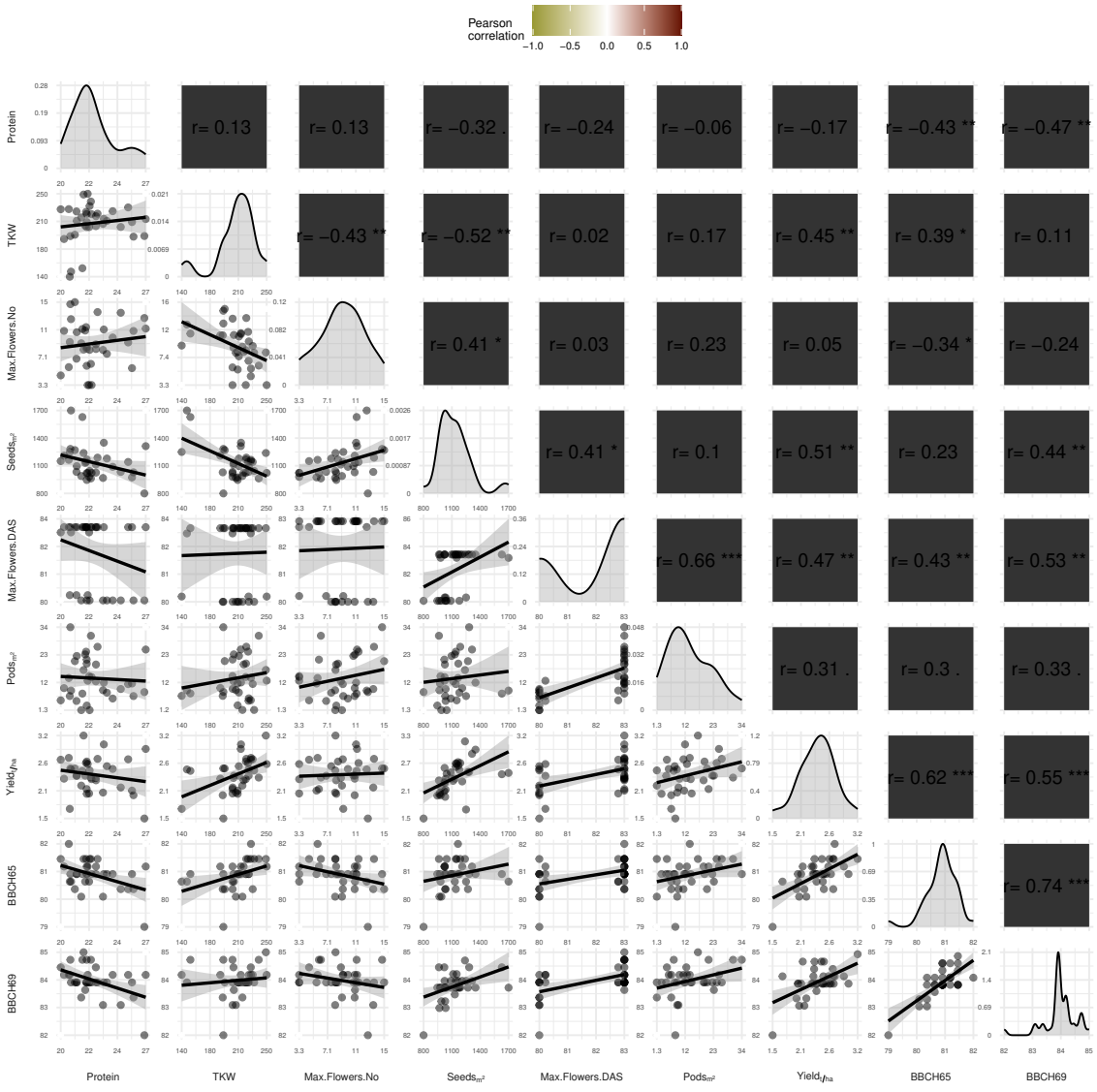

Figure S.7. Correlation plot of all variables from Year 2023. Darker values indicate higher correlations. Significance is shown with stars, where *p<0.05; **p<0.01; ***p<0.01

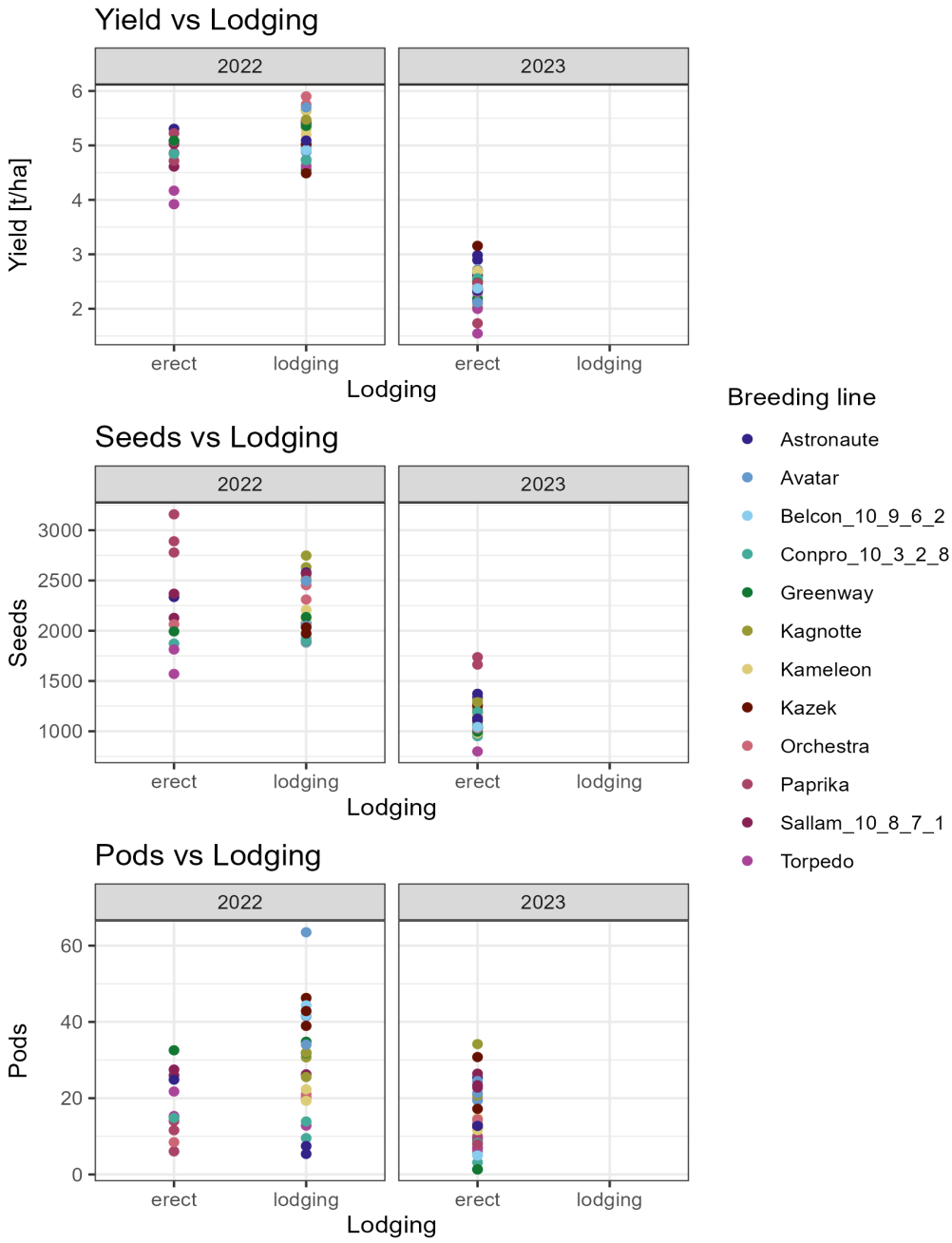

Figure S.8. Lodging in 2022 and 2023 compared to number of pods, seeds and yield.